DYNAMIC AND STATIC MEASUREMENTS OF SMALL STRAIN MODULI OF TOYOURA SAND

Yukika TSUTSUMI[1], Manuel Builes[2], Takeshi SATO[3] and Junichi KOSEKI[4]

ABSTRACT: A series of triaxial tests were performed on specimens made of Toyoura sand having different dry densities. Very small unloading/ reloading cycles were applied to obtain "static" Young's modulus. Furthermore, as the "dynamic" measurements, two types of wave propagation techniques were applied; one is using bender elements, and the other is using piezoelectric actuators to excite primary and secondary waves. Based on these static and dynamic measurements, 1) the difference among the three types of dynamic measurements, 2) the relationships between the dynamic and static measurement results and 3) the effects of stress state-induced anisotropy and dry densities of the specimens are mainly discussed.

Key Words: Triaxial test, Small strain cyclic loading, Primary wave velocity, Secondary wave velocity, Accelerometer, Bender element, Young's modulus, Shear modulus

INTRODUCTION

It is well known that the ground deformation under the normal working condition is generally less than 0.1% of strain. In soil mechanics, it is normally assumed that the ground consists of a continuum and that its behavior is linear and recoverable within a very small strain range i.e. lesser than 10^{-3} % (Tatsuoka & Shibuya, 1992). Therefore, "elastic" deformation properties of soil like Young's modulus and shear modulus play an important role in designing civil engineering structures. In order to obtain these parameters through in-situ tests, it is common to use PS logging by cross hole, down hole and suspension sonde methods, while as laboratory tests to evaluate these properties, resonant column, torsional shear and triaxial tests as well as bender elements are commonly used.

In this study, Toyoura sand specimens having different dry densities were subjected to triaxial tests. Very small unloading/ reloading cycles were applied at several stress states, and strains were measured locally using local deformation transducers at the side surface of the specimen. This method is called as "static" herein. For the "dynamic" measurement, two types of wave propagation techniques were applied. One was using bender elements which have been widely used for laboratory testing. The other was composed of piezoelectric actuators and accelerometers made of ceramics, which was developed by Anh Dan et al. (2002).

Based on these static and dynamic measurements, elastic moduli are compared with each other, especially focusing on the following issues; 1) the difference among the three types of dynamic measurements, 2) the relationships between the dynamic and static measurement results and 3) the effects of stress state-induced anisotropy and dry densities of the specimens.

[1] Technical staff, Institute of Industrial Science, University of Tokyo
[2] Former graduate student, Department of Civil Engineering, University of Tokyo
[3] Research Associate, Institute of Industrial Science, University of Tokyo
[4] Professor, Institute of Industrial Science, University of Tokyo

TESTED MATERIAL, EQUIPMENT AND TEST PROCEDURES

Specimen preparation and apparatus

The tested material was Toyoura sand (mean grain diameter, D_{50}= 0.21 mm, density of solid particles, ρ_S = 2.656g/cm^3, maximum void ratio, e_{max} = 0.992, and minimum void ratio, e_{min} = 0.632) having relatively uniform gradation as shown in **Figure 1**. Air dried Toyoura sand particles were pluviated through the air to prepare a cylindrical specimen with dimensions of 5 cm in diameter and 10 cm in height. Specimens having relative densities, Dr, of about 50 and 80 % (the dry density ρ_d equal to 1.454 and 1.553-1.568 g/cm^3, respectively) were prepared to study the effect of density.

For the triaxial apparatus employed in this study, an AC servo motor was used in the loading system so that very small unloading/ reloading cycles (cyclic loading) under strain control could be applied accurately to the specimen in the vertical direction. To measure the vertical stress, σ_1, a load cell is located just above the top cap inside the triaxial cell in order to eliminate the effects of piston friction (Tatsuoka, 1988). The vertical strain ε_1 was measured not only with the external displacement transducer but also with a pair of vertical local deformation transducers (LDTs) (Goto et al., 1991), located on opposite sides of the specimen. The horizontal stress σ_3 was applied through the air in the cell, which was measured with a high capacity differential pressure transducer (HCDPT).

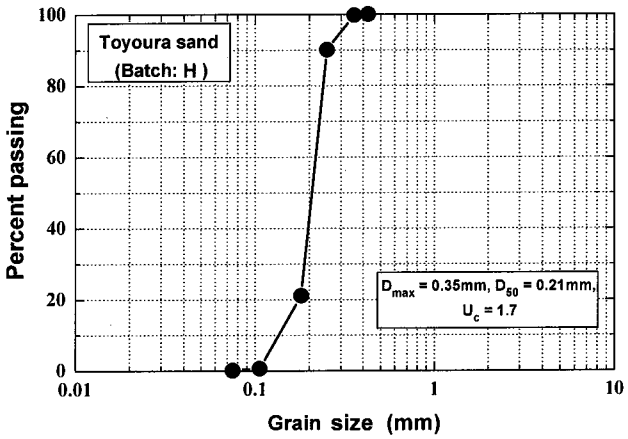

Figure 1. Grain size distribution of Toyoura sand

Dynamic measurement using piezoelectric actuators and accelerometers

To generate primary wave (P wave) and secondary wave (S wave), a special type of wave source (called trigger) was employed (**Figure 2a**). It was composed of a multi-layered piezoelectric actuator made of ceramics (dimensions of 10 mm x 10 mm x 20 mm, mass of 35 grams and a natural frequency of 69 kHz), and a U-shaped thick steel bar to provide reaction force. Triggers were used in pairs to apply large excitation equally (Builes et al., 2004). To receive the dynamic waves, piezoelectric accelerometers (cylindrical in shape with a diameter of 3.6 mm, a height of 3 mm, a mass of 0.16 grams, and natural frequency of 60 kHz) as shown in **Figure 2b** were used.

P wave is a vertically-transmitting compression wave given by a couple of triggers set on the top cap, as denoted "PT" in **Figure 3**. S wave is a vertically-transmitting tortional wave given by the other couple of triggers set to the opposite sides of the top cap, "ST" in **Figure 3**. These dynamic waves were received by three pairs of accelerometers which were glued on the side surface of the specimen at two different heights as shown in **Figure 3** ("P" and "S" in the circles, respectively). One pair on "side A" was for P wave measurement to evaluate Young's modulus, and the other two pairs on both sides A and B were for S wave measurement to evaluate shear modulus.

Dynamic measurement using bender elements

Bender Elements are small piezo-electrical transducers which either bend as an applied voltage is changed or generate a voltage as they are bent (**Figure 4a** and **Figure 4b**). In this study, electrical signal was sent to the bender element fixed to the top cap to use it as a trigger. It was set vertically, shown as "BE" in **Figure 3**, so that it generates vertically-transmitting horizontally-polarized waves, equivalent to the S wave triggered by the piezoelectric actuators, and they were received by the other bender element fixed to the pedestal.

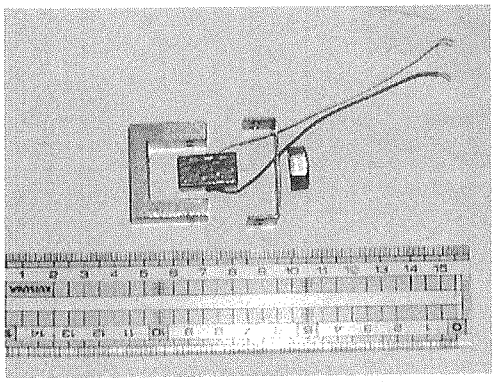

Figure 2a. Components of a trigger

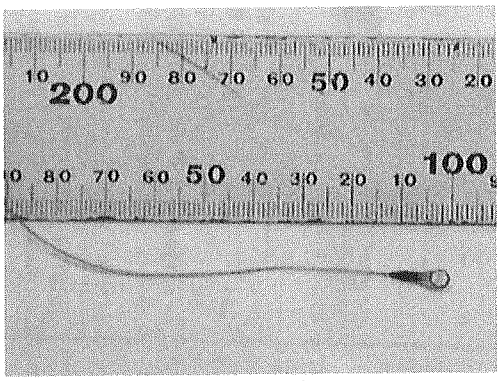

Figure 2b. Accelerometer

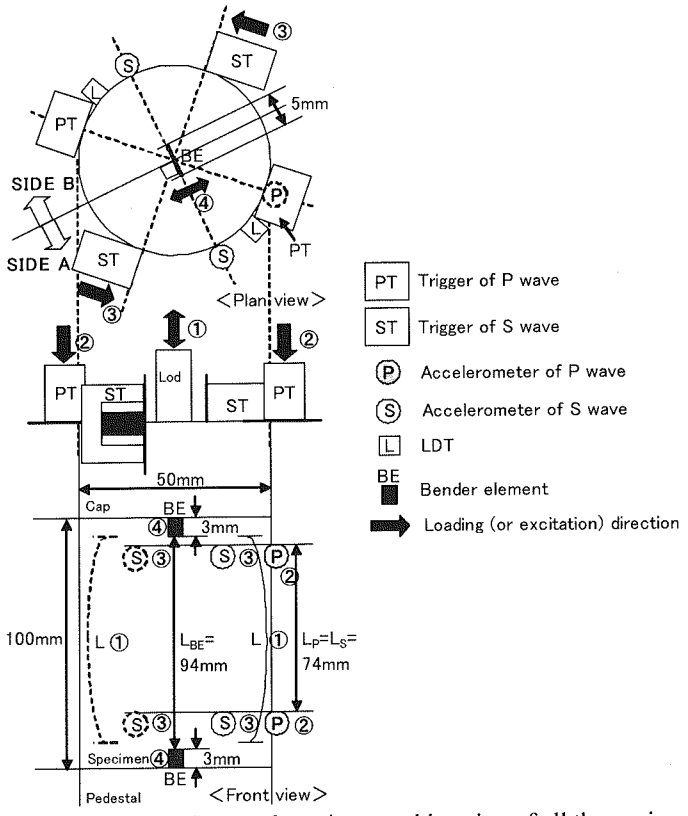

Figure 3. Schematic figure of specimen and location of all the equipment

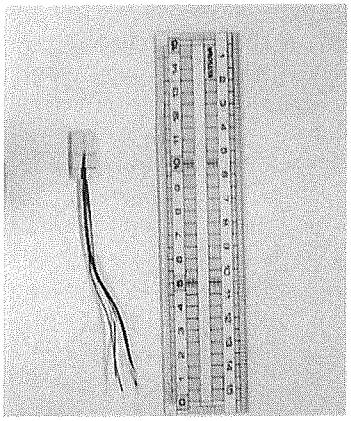

Figure 4a. Bender element

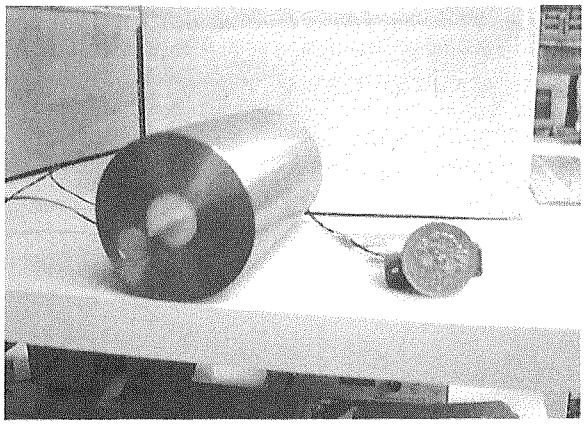

Figure 4b. Set-up condition of bender element (at pedestal)

Recording techniques of dynamic waves

A digital oscilloscope was employed to record electrical outputs from the accelerometers and bender elements with an interval of 10^{-6} sec. To obtain clear signals, a stacking (averaging) technique which had been originally installed in the oscilloscope was introduced instead of using any filtering methods (Maqbool et al., 2004 b). The number of stacking was 256 with the bender elements and 128 with the accelerometers.

Testing procedures

A flow chart of the procedures for each measurement is shown in **Figure 5**. Each specimen was kept under air-dried condition and subjected to isotropic or anisotropic consolidation. During anisotropic consolidation, the ratio of the horizontal stress to the vertical one was kept at 0.5. After the vertical stress, $\sigma_v(=\sigma_1)$, reached to 50, 100, 200, and 400 kPa, the dynamic and static measurements were conducted.

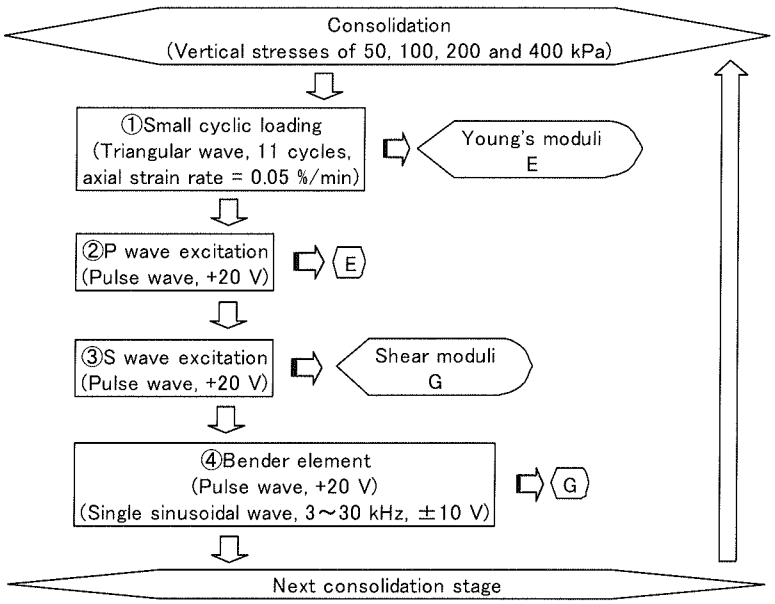

Figure 5. Flow chart of testing procedures for each measurement

First, small cyclic loading (11 cycles, triangular wave, axial strain rate, $\dot{\varepsilon}_V$, equal to 0.05%/min) was applied to evaluate vertical Young's modulus statically. Second, electric voltage of +20 volt in the form of single pulse were supplied to the triggers for exciting P and S waves to evaluate Young's modulus and shear modulus, respectively. At last, single pulse wave (+20 volt) and single sinusoidal waves (± 10 volt) at different frequencies which range from 3 to 30 kHz were supplied to the bender element to evaluate shear modulus.

Under these conditions, three tests were performed. The first test was under isotropic consolidation with Dr of about 50%, named "IC50"; the second was under isotropic consolidation with Dr of about 80% (IC80), and the last was under anisotropic consolidation with Dr of about 80% (AC80).

EVALUATION PROCEDURES OF STATIC AND DYNAMIC MODULI

Evaluating elastic modulus

Typical stress-strain relationship during a small vertical loading cycle is shown in **Figure 6**. At each stress state, the stress-strain relationship was fitted by a linear function, and the small-strain vertical Young's modulus, E_S, was evaluated from its inclination.

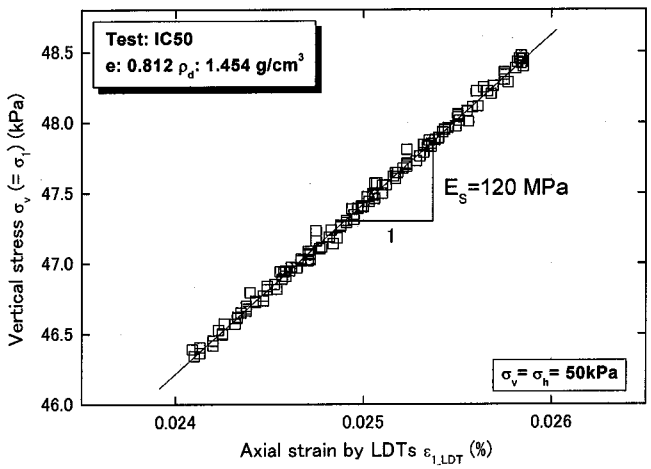

Figure 6. Typical stress-strain relationship during a small vertical loading cycle

In computing dynamic Young's modulus E_D, we assumed that unconstrained compression waves were generated because the top cap touched the whole cross-section of the specimen that was with free side boundaries. The P wave velocity V_P is directly related to the small-strain vertical Young's modulus of the material by the dynamic measurement as:

$$E_D = \rho V_P^2 \tag{1}$$

where ρ is the dry density of the specimen. In the same manner, dynamic shear modulus G_D was evaluated from the S wave velocity V_S as:

$$G_D = \rho V_S^2 \tag{2}$$

The compression wave velocity V_P, shear wave velocities measured with the accelerometers and the bender element, $V_{S\_Acc.}$ and V_{S_BE}, respectively were calculated by the same equation as follows:

$$V = L/t \tag{3}$$

Here the wave velocity "V" can be replaced with "V_P", "$V_{S\_Acc.}$" or "V_{S_BE}", while substituting the distance "L" and the corresponding travel time "t" with L_P, L_S, or L_{BE} and t_P, t_S, or t_{BE}, respectively. The distances L_P, L_S, and L_{BE} are the differences in the vertical locations between each pair of accelerometers or bender elements as defined in **Figure 3**.

In these evaluations, it was assumed that the dry density was kept constant as the volume change due to consolidation of the air-dried specimen could not be measured. On the other hand, the effect of vertical deformation obtained from LDTs at each stress state was considered in the calculation of the distances L_P, L_S, and L_{BE}.

Travel time definitions

Based on the records of accelerometers measuring P and S wave excitations, the time difference in the first wave arrival between the upper (input) and the lower (output) accelerometers was computed. Although there are several ways to detect the travel time (e.g. Maqbool et al., 2004 a), in this study, two types of simple definitions were employed.

In the first technique, as shown in **Figure 7**, "t" was computed based on the first rising points of the input and output waves. It will be hereafter called as "first rise to first rise" technique and denoted as "t_{rise}". In this method, a problem lies with the decision of evaluation of the first rising point in both signal records. The outcome may depend on observer's judgment.

In the second technique, "t" was determined using the first peak points of input and output waves as shown in **Figure 7**. It will be called "peak to peak" technique and denoted as "t_{pk}". In this technique, the observer has to decide the correct peak points. In most of the cases, it's easier to do so than deciding the correct rising points, while there were some exceptions in the P wave records (as will be discussed later).

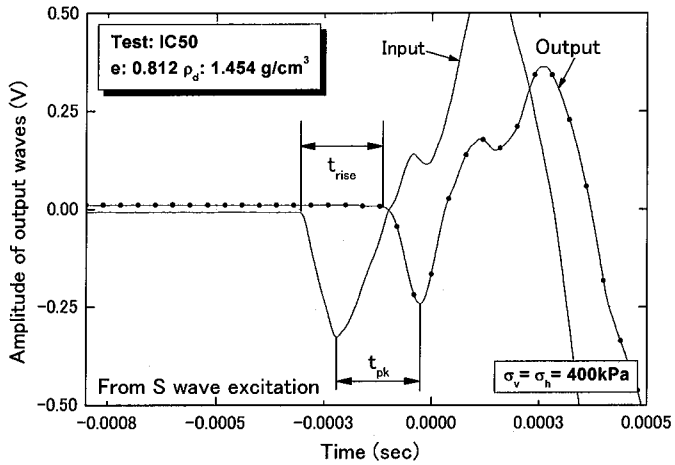

Figure 7. Definitions of travel time "t" using; first rise and first peak techniques

In case of bender elements, the time difference between the input wave to the bender element at the top cap and the output one from the bender element at the pedestal was used, since it was confirmed in the relevant study that the bender element used as the trigger responds against the input signal without any significant time lag. Travel time definitions are the same with the one explained above.

Figure 8 shows some time-history data from the bender element under the vertical stress equal to 200 kPa in test AC80. A single pulse and some representative single sinusoidal wave records are included. The upper graph on the left presents all the input wave records, while the others show each output wave record. From the output records, the first rising point can not be identified clearly. Besides this,

although all the input waves were transmitted in the same direction, it seems that the first peak with the pulse wave excitation is on the negative side, while all of the first peaks with the sinusoidal waves are to the opposite, i.e. positive. In spite of such kinds of difficulties in evaluating the travel time, the first rising points or peak points were determined rather empirically, while referring to the data obtained under different input wave conditions as well.

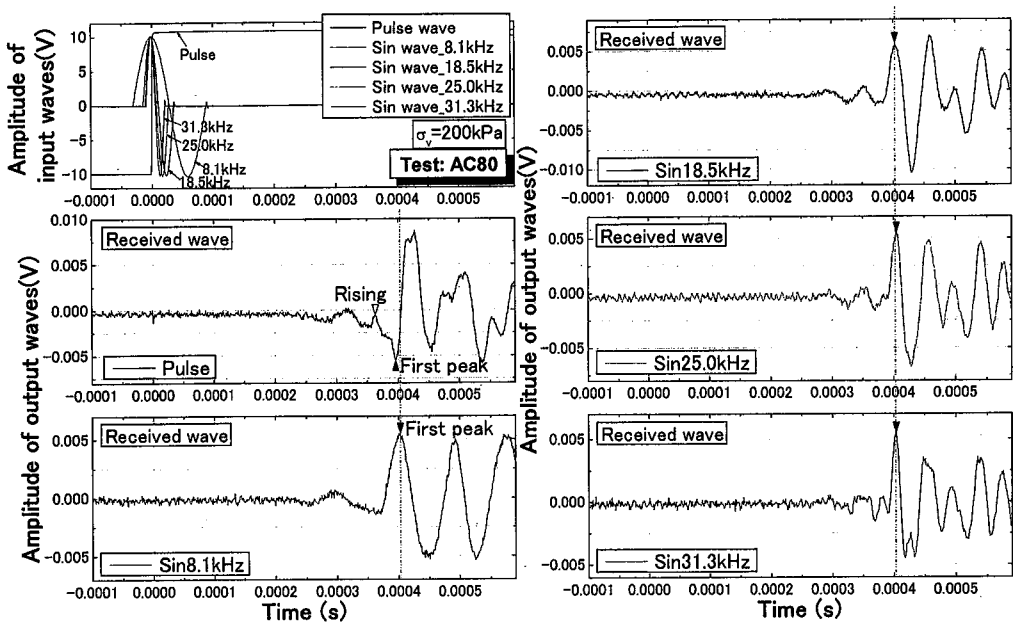

Figure 8 Time-history data from bender element

TEST RESULTS AND DISCUSSIONS

To compare among different measurement techniques, the Young's moduli obtained from small cyclic loading and P wave excitation, E_v, are converted to shear moduli G_{vh}. In general, isotropic elasticity modeling is employed for the conversion by using the following equation:

$$G_{vh} = \frac{E_v}{2(1+\nu)} \tag{4}$$

where ν: Poisson's ratio (set equal to the value of ν_0, as will be shown later)

On the other hand, another equation based on an anisotropic elasticity modeling was proposed by Tatsuoka et al. (1999). Since this model can consider both the inherent and stress state-induced anisotropy, this equation is employed in this study to consider only the stress state-induced anisotropy. The equation and the settings of each coefficient are as follows:

$$G_{vh} = \frac{E_v}{2(1+\nu_0)} \frac{2(1-\nu_0)}{1+aR^n - 2\sqrt{a}\cdot R^{n/2}\cdot \nu_0} \tag{5}$$

where ν_0: reference Poisson's ratio (set as 0.17, by referring to Hoque and Tatsuoka(1998))

a: coefficient on the degree of inherent anisotropy (set as 1.0, by neglecting the possible effect of inherent anisotropy),

R: stress ratio (= σ_v/σ_h)

n: coefficient on the degree of stress-state dependency (set as 0.44, referring to the results from small cyclic loading)

It should be noted that Equation (4) can be drawn from Equation (5) when isotropic conditions are applied to the value of a and R, i.e. a = R = 1.0.

Relationships between shear moduli and the stress levels based on all the static and dynamic measurements in each test are shown in **Figure 9** to **Figure 11**. In the legend of these figures, "Peak" or "Rising" means that "t_{pk}" or "t_{rise}" was selected as the travel time. The results obtained by bender elements with sinusoidal waves (denoted as "Bender elements_Sin_Peak") are based on the average value evaluated with clear wave records at different frequencies. As clearly seen in **Figures 9** to **11**, shear moduli increased with the increase in the stress levels, and their relationships were linear in logarithmic scale. In general, the values of shear moduli of denser specimens in the tests IC80 and AC 80 were larger than those of looser specimen in the test IC50. It should be noted that all the values of shear moduli converted from the static Young's moduli, denoted as "Cyclic loading" in these figures coincided with the lower bound of the dynamic measurements, i.e. all the values by dynamic measurements were larger than those by the static measurements. Detailed discussion on the differences between static and dynamic measurements will be made later.

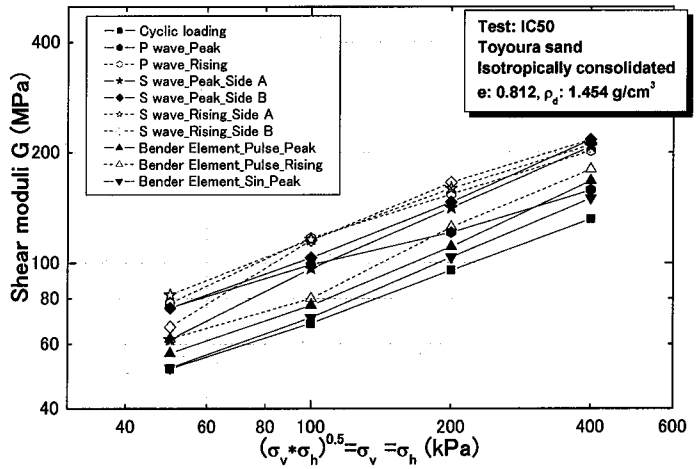

Figure 9 Relationships between shear moduli and stress levels (test IC50)

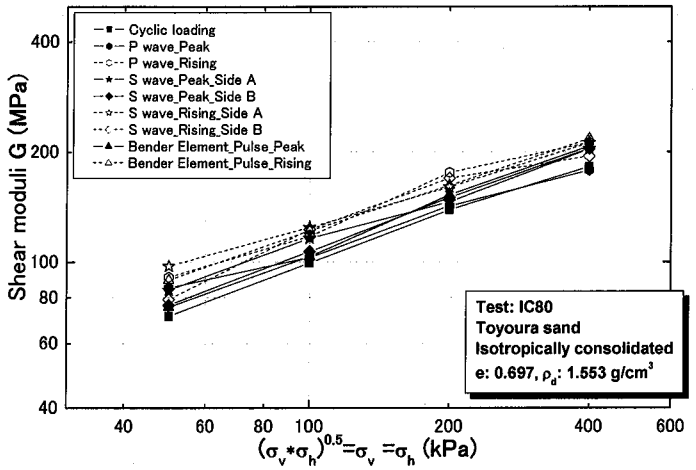

Figure 10 Relationships between shear moduli and stress levels (test IC80)

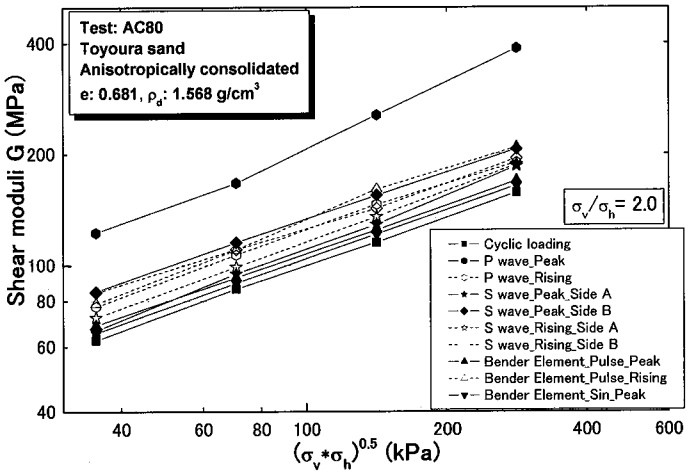

Figure 11 Relationships between shear moduli and stress levels (test AC80)

In every test, the shear moduli by S wave excitation measured on both sides A and B (refer to **Figure 3**) can be regarded as similar to each other under each travel time definition. Accordingly, averaged values measured on both sides will be regarded as the representative of whole the specimen and compared with those by other measurements in the latter discussions.

Comparison between S wave excitation using triggers and bender elements

The shear moduli values obtained by S wave excitation using the triggers, G_{Sw} (indicated with a notation "Sw"), and the bender elements, G_{BE} (indicated with a notation "BE"), in all the tests are compared in **Figure 12**. The general trends on stress state dependency of G_{Sw} and G_{BE} were consistent to each other. However, it could be seen that the G_{Sw} values were almost similar at the same stress levels irrespective of the different densities of the specimens, while the G_{BE} values of denser specimens in the tests IC80 and AC80 were larger than those of looser one in the test IC50. As a result, the G_{Sw} and G_{BE} values showed good agreement with each other with the denser specimens, while the difference between the G_{Sw} and G_{BE} values amounted up to 40 % with the looser specimen at each stress level.

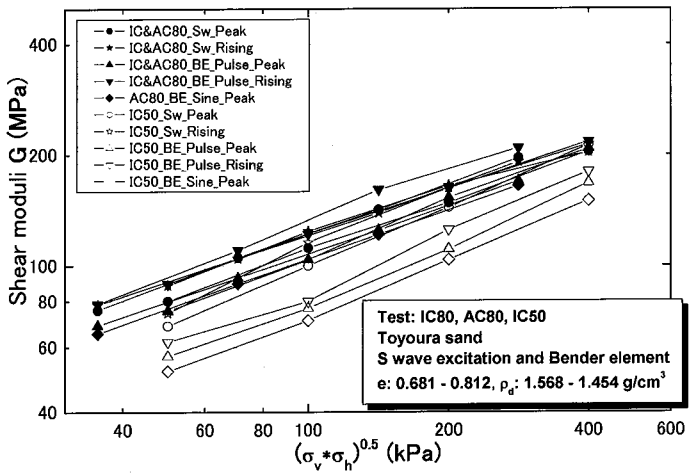

Figure 12. Comparison between S wave excitation using actuators and bender elements

Comparison between P wave and S wave measurements

The G_{Sw} values and the shear moduli values, G_{Pw}, that are converted from vertical Young's moduli obtained by P wave excitation are compared in **Figure 13**. It was observed that stress state dependencies of G_{Pw} calculated based on t_{pk}, denoted as "Pw_Peak" in this figure, were not consistent with the others. In addition, the G_{Pw} values under this definition in the test AC80 were much larger than the other results.

As an example, time-history data from P wave measurement at each stress level in the test AC80 are presented in **Figure 14**. On both input and output records, some disturbances in the wave forms at the peak in the first half cycle could be observed, and their shapes changed continuously as the confining pressure increased. These properties should have affected the travel time evaluations and thus caused the above inconsistent values of G_{Pw}. The reason for these disturbances of the first half cycles would be wave generation by the couple of triggers that may not simultaneously. Therefore, the results from dynamic measurements based on t_{rise} are employed in the following discussions.

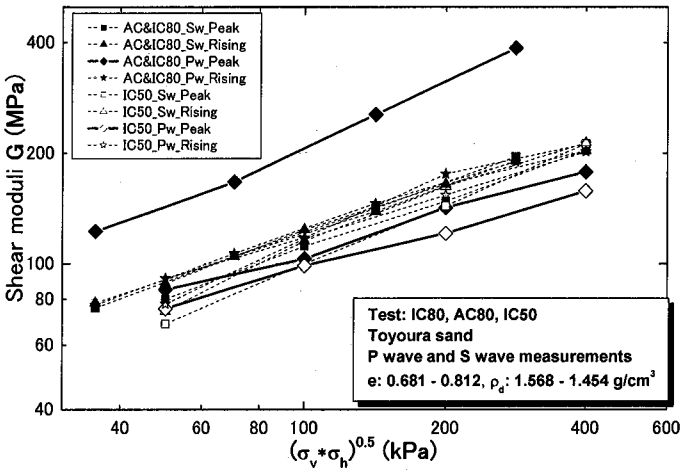

Figure 13. Comparison between P wave and S wave measurements

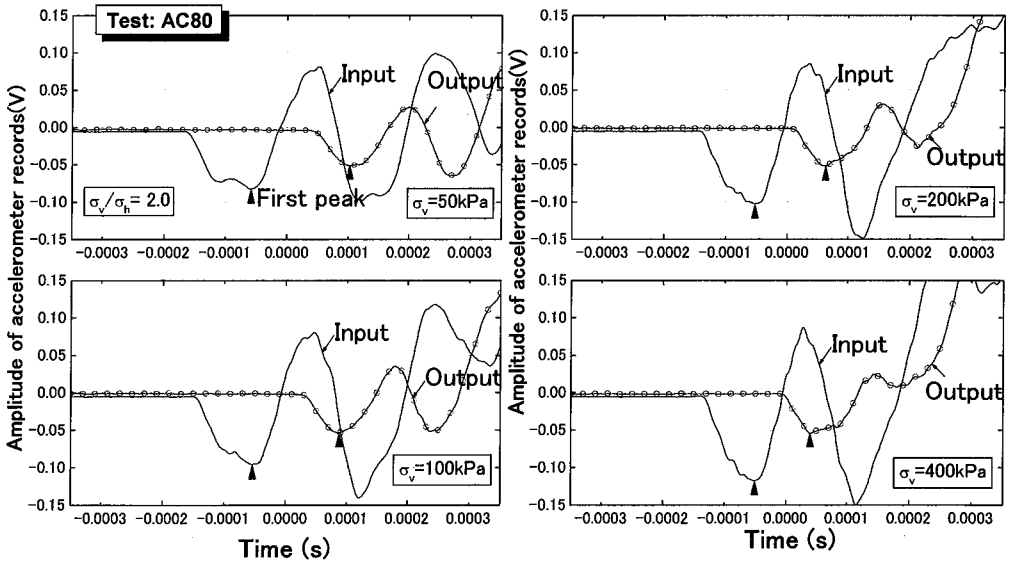

Figure 14. Time-history data from P wave measurement in the test AC80

Comparison between static and dynamic measurements

For comparison between the dynamic and static measurements, the vertical Young's moduli obtained by P wave excitation, E_{Pw} calculated with t_{rise} (denoted as "Pw_Rising"), and the static measurements, E_S (denoted as "Cyclic loading"), are shown in **Figure 15**. It could be clearly observed that the E_S values under the same dry density of the specimens in the tests IC80 and AC80 were almost equal to each other at each vertical stress level irrespective of the different horizontal stresses, and the E_S values of looser specimen in the test IC50 were consistently smaller than those of denser specimens. On the other hand, the E_{Pw} values were almost similar at each vertical stress level irrespective of the different densities of the specimens and horizontal stresses. Consequently, the dynamic moduli of denser specimens were larger than the static moduli by about 20 %, while the difference between the dynamic and static moduli of looser one became as larger as 60 %.

The reason for these phenomena would be that the dynamic wave does not reflect the overall cross-sectional property of the specimen but travels through the shortest path made by interlocking of soil particles, resulting into larger elastic moduli as compared to those by the static measurement (Tatsuoka and Shibuya, 1991; Maqbool et al, 2006). With this inference, it would be also possible that the difference in the elastic moduli would increase with the decrease in the dry density, since looser specimens would have larger structural or microscopic heterogeneity than denser ones. However, it is generally recognized that the differences between dynamic and static measurements on fine uniform sands like Toyoura sand are very small and negligible as compared to those on well graded materials having large particles.

In addition to the above differences between static and dynamic measurements, the dynamic shear moduli by the bender elements in this study showed different tendency from the other dynamic measurements. To clarify the relationships between the dynamic and static measurements more in detail, further investigations are required including the issue of proper determination of travel time from the records of P wave and bender elements.

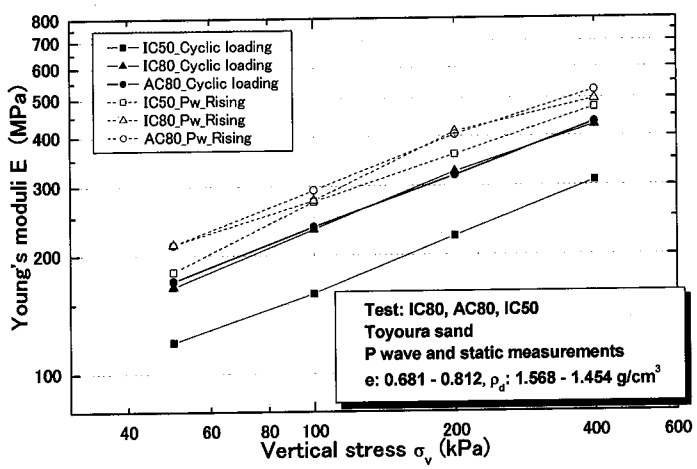

Figure 15. Comparison between static and dynamic measurements

Effect of stress state-induced anisotropy

To discuss the effect of stress state-induced anisotropy, as shown in **Figure 16**, the shear moduli G_{Sw} are regarded as the references here (denoted as "Sw_Rising"), and are compared with the other shear moduli, G_S and G_{Pw}, that are converted from statically and dynamically measured Young's moduli in the tests IC80 and AC80. It could be observed that the G_{Pw} values in the test IC80 using Equation (4) (denoted as "IC80_Pw_Rising_Eq.(4)") showed good agreement with the G_{Sw} values, while the G_{Pw}

values in the test AC80 using Equation (4) (denoted as "AC80_Pw_Rising_Eq.(4)") were different from the other dynamic measurements. By employing Equation (5), however, the G_{Pw} values in the test AC80 (denoted as "AC80_Pw_Rising_Eq.(5)") coincided with the other results since the stress state-induced anisotropy was properly considered. In the same manner, the G_S values in the test AC80 became almost the same as the G_S values in the test IC80 by using Equation (5) instead of Equation (4). Comparisons described above demonstrate the importance of considering the effects of stress state-induced anisotropy in comparing the elastic properties defined on different planes.

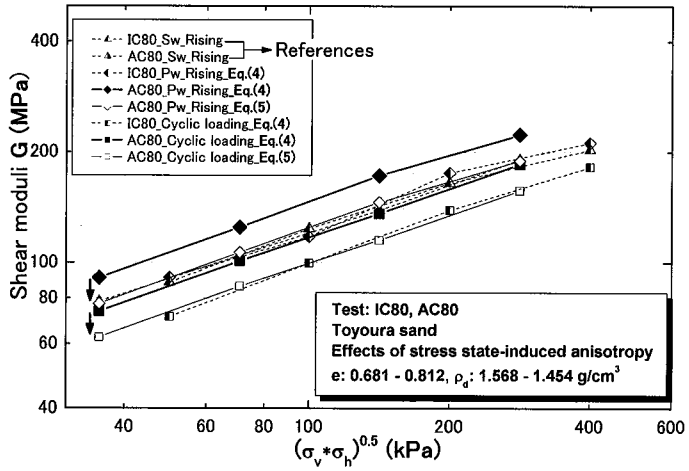

Figure 16. Effect of stress state-induced anisotropy

CONCLUSIONS

The following conclusions can be drawn from the results presented in this study.

1. Dynamic measurement results in terms of shear moduli based on the secondary and primary wave velocities using piezoelectric actuators showed good agreements to each other, and these values were rather similar irrespective of the different densities of the specimens.
2. Dynamic Young's moduli based on the primary wave velocity were larger than those by static measurement, and the difference between them increase with the decrease in the densities of the specimens.
3. Dynamic measurement results obtained by the bender elements showed the dependency on the densities of the specimens unlike the other dynamic measurement results. To clarify the relationships between dynamic and static measurements more in detail, further investigations are required including the issue of proper determinations of travel time from the records of P wave and bender elements.
4. By considering the effect of stress state-induced anisotropy, the shear moduli based on the secondary wave velocity and the converted shear moduli from vertical Young's moduli coincided with each other both on the dynamic and static measurements. It would demonstrate the importance of considering the effects of stress state-induced anisotropy in comparing the elastic properties defined on different planes.

ACKNOWLEDGMENT

Thanks to detailed information provided by Dr. Satoshi Yamashita at Kitami Institute of Technology, installation of bender elements to the triaxial apparatus employed in the present study could be made possible. The authors want to express deep gratitude to Dr. Sajjad Maqbool, former PhD student at the University of Tokyo, for his help in using dynamic wave measurement techniques.

REFERENCES

AnhDan, L.Q., Koseki, J. and Sato, T. (2002). "Comparison of Young's moduli of dense sand and gravel measured by dynamic and static methods." Geotechnical Testing Journal, ASTM, Vol.25, No.4, pp.349-368.

Builes, M., Maqbool S., Sato T. and Koseki J. (2004). "Comparison of static and dynamic methods to evaluate Young's modulus of dry Toyoura sand" Proceedings of the Sixth International Summer Symposium, JSCE, Saitama, pp. 229-232.

Goto, S., Tatsuoka, F., Shibuya, S., Kim, Y.S. and Sato, T. (1991). "A simple gauge for local small strain measurements in the laboratory." Soils and Foundations, No.1, Vol.31, pp.169-180.

Hoque, E and Tatsuoka F. (1998). "Anisotropy in the elastic deformation of materials" Soils and Foundations, 38-1, pp. 163-179.

Maqbool, S., Koseki, J. and Sato, T. (2004) a. "Effects of compaction on small strain Young's moduli of gravel by dynamic and static measurements" Bulletin of ERS (Earthquake Resistant Structure Research Center), IIS, University of Tokyo, No.37, pp. 41-50.

Maqbool, S., Sato, T. and Koseki, J. (2004) b. "Measurement of Young's moduli of Toyoura sand by static and dynamic methods using large scale prismatic specimen" Proceedings of the Sixth International Summer Symposium, JSCE, Saitama, pp. 233-236.

Maqbool, S., Tsutsumi, Y., Koseki, J., and Sato T. (2006), "Effect of lubrication layers on small strain stiffness of dense Toyoura sand" , International Symposium on Geomechanics and Geotechnics of Particulate Media, Japan. (Submitted for possible publication)

Tatsuoka, F. (1988). "Some recent developments in triaxial testing systems for cohesionless soils." Advanced Triaxial Testing of Soils and Rock, STP 977, ASTM, Philadelphia, pp.7-67.

Tatsuoka,F. and Shibuya,S. (1991), "Deformation characteristics of soils and rocks from field and laboratory tests", Keynote Lecture for Session No.1, Proc. of the 9th Asian Regional Conf. on SMFE, Bangkok, Vol.II, pp.101-170.

Tatsuoka, F. and Shibuya, S. (1992). "Deformation characteristics of soils and rocks from field and laboratory tests." Proc. of 9th Asian Regional Conference of SMFE, Bangkok, Vol. 2, pp.101-170.

Tatsuoka, F., Ishihara, M., Uchimura, T. and Gomes Correia, A. (1999). "Non-linear resilient behavior of unbound granular materials predicted by the cross-anisotropic hypo-quasi-elasticity model" Unbound Granular Materials, Balkema, pp. 197-204.